

UC Irvine

UC Irvine Previously Published Works

Title

Bayesian optimization of laser-Compton x-ray sources for medical imaging applications

Permalink

<https://escholarship.org/uc/item/1k7713sf>

ISBN

9781510660311

Authors

Reutershan, Trevor
Effarah, Haytham H
Barty, CPJ

Publication Date

2023-04-07

DOI

10.1117/12.2654377

Copyright Information

This work is made available under the terms of a Creative Commons Attribution License, available at <https://creativecommons.org/licenses/by/4.0/>

Peer reviewed

Bayesian optimization of laser-Compton x-ray sources for medical imaging applications

Trevor Reutershan^{*a,b}, Haytham H. Effarah^{a,b}, C.P.J. Barty^{a,b}

^aBeckman Laser Institute and Medical Clinic, University of California – Irvine, Irvine, CA, USA 92697; ^bDepartment of Physics and Astronomy, University of California – Irvine, Irvine, CA, USA, 92697

*treuters@uci.edu

ABSTRACT

Laser-Compton x-ray sources have many advantages over traditional x-ray tubes for use in medical imaging due to their monoenergetic energy spectrum, tunability, high-flux, and low-dose potential. These properties can specifically be taken advantage of in the context of K-edge subtraction (KES) imaging. Previous optimization approaches are time-consuming by scanning over high-dimensional parameter spaces. Here, we show how a Bayesian optimization routine optimizes LCS source parameters in only a fraction of the computational time. Using this approach, we found a configuration that produces non-inferior image quality in KES mammography compared to a previously optimized direct energy tuning technique. Moreover, a successfully optimized implementation of scanning K-edge subtraction imaging was realized applying this Bayesian approach.

Keywords: laser-Compton scattering, K-edge subtraction, machine learning, Bayesian optimization, dual energy imaging, x-ray, mammography

1. INTRODUCTION

Laser-Compton scattering (LCS) x-ray sources are an emerging technology for use in medical imaging [1-3]. These sources provide benefits over the traditionally used and over 125-year-old x-ray tubes in many ways, including: significantly narrower energy bandwidths, direct energy tuning capability with a large dynamic range from 10's of keV into the MeV range, intense collimation, and the potential for high fluxes.

Despite these advantages, the optimization of LCS sources for medical imaging applications has been largely ignored but it is a necessary step towards clinical implementation. Optimization of LCS sources is not a straight-forward task, as there are several optimizable parameters (electron beam energy and energy spread, pointing jitter, collimation aperture shape and size, etc. ...) that all effect a nonlinear output spectrum. Here we show how Bayesian optimization can be used to find the optimal settings in a large LCS source parameter space, in particular for a K-edge subtraction (KES) imaging application.

1.1 Laser-Compton Scattering

Medical x-ray imaging exclusively utilizes x-ray tubes. This technology takes electrons with peak energy up to a specified voltage potential, usually between 20 and 160 kVp, and strikes an anode target material. The charged electrons undergo deceleration by emitting electromagnetic radiation in a process known as bremsstrahlung. The energies of the scattered photons are broadly distributed from zero up to the kinetic energy of the electron. While useful, this technology has the significant drawback of large energy bandwidths introducing low energy photons that provide no imaging capability and purely add dose to the patient.

LCS sources are an emerging technology that overcome this broad bandwidth limitation. They operate by colliding a relativistic electron beam head on with intense laser pulses [4,5]. In this configuration, the energy of the scattered photon, E_γ , can be represented by the following formula [6],

$$E_\gamma = \frac{4\gamma^2}{1 + \gamma^2\theta^2 + 4\gamma k_0 \lambda_c} E_L \quad (1)$$

Here, E_L is the energy of the incident laser photons, θ is the scattering angle, k_0 is the wavenumber of the incident laser photon, γ is the Lorentz factor of the electron, and λ_c is the reduced Compton wavelength.

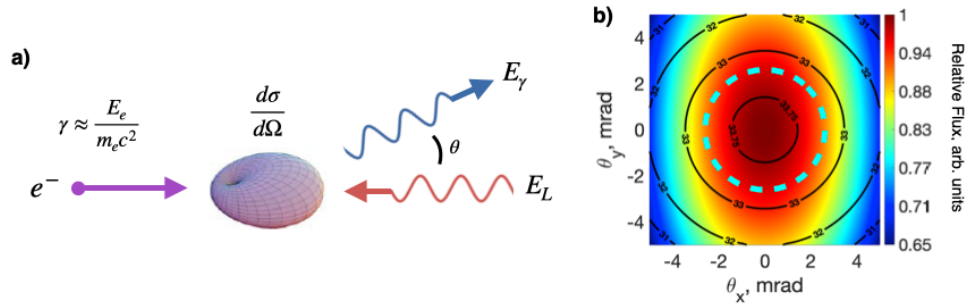


Figure 1. a) Illustration of the electron-laser scattering occurring in LCS sources. The most typical orientation is a head-on collision due to it enabling narrow on-axis energy bandwidths. The intensity distribution imaged here represents a dipole Compton radiation pattern. b) Energy-angle-intensity distribution of a LCS x-ray source. The colormap is the relative intensity, with the largest intensity being center axis. The circular contours are of the mean energy in keV. The dashed light blue circle represents the K-edge energy of iodine.

When this interaction is performed between bunches of electrons and pulses of photons, the result is a spatial energy-intensity profile of the scattered radiation. Each unit in the solid angle has a local energy bandwidth that is characteristic of the electron beam and laser pulse properties. Figure 1b shows the x-ray distribution from such sources and a sample of which is used in this study. These systems are designed to have 0.1% on-axis energy bandwidth ($\Delta E/E$, FWHM). The bandwidth may be adjusted with simple collimation by excluding the lower energy photons that scatter away from the center axis.

1.2 K-Edge Subtraction Imaging

As an example of the Bayesian algorithm’s use case, we apply it to an application of a LCS-KES imaging problem. K-edge subtraction imaging is a contrast-based dual-energy modality that takes advantage of the large discontinuous change in the contrast element’s 1s shell photoabsorptive cross-section (referred to as the K-edge). By taking an image using x-rays with energy just above the K-edge energy (33 keV for iodine) and another image just below this energy, subtraction of the two images will remove distracting background tissue and leave enhancement at the contrast agent only.

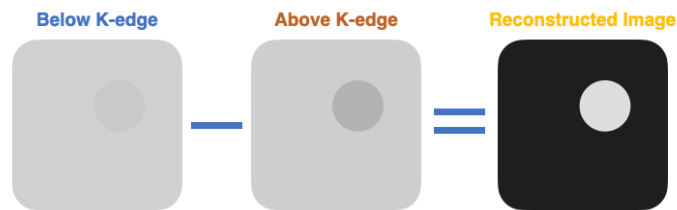


Figure 2. Cartoon illustrating how post-processing in K-edge subtraction removes distracting background features and leaves enhancement at the site of contrast uptake.

Clinical mammography systems that use this technique are currently available and have been shown to be as sensitive as contrast enhanced MRI at detecting breast cancer [7]. Figure 3b compares the spectrum of GE’s Senobright, a clinical contrast-enhanced dual-energy mammography (CEDEM) machine available for purchase, to that of a 1.5% bandwidth ($\Delta E/E$, FWHM) LCS energy spectrum. The best and most ideal spectra to use for a KES image would be a monoenergetic spectrum just above and below the iodine K-edge. The clinical CEDEM machine is far from ideal with large bandwidths that are far from the K-edge. The ideal scenario can be closely attained using a LCS source’s narrow quasi-monoenergetic

bandwidths, thereby maximizing contrast and minimizing background. A further advantage the LCS source has is that it lowers the dose by excluding unnecessary low energy photons that do not make it through the patient.

Because the energy is dependent on the scattering angle in a LCS source, energies that are both above and below a contrast element's K-edge may be present simultaneously and separated in space. This enables a single tuning of the electron beam energy be made and translation of the object through the X-ray source exposes it to both energies in a process we refer to as scanning K-edge subtraction (SKES) [8,9]. Such a configuration eliminates the need for two separate energy tunings making the imaging time faster. Application of the Bayesian optimization process to SKES imaging is of interest in this paper as a validation of the algorithm's use.

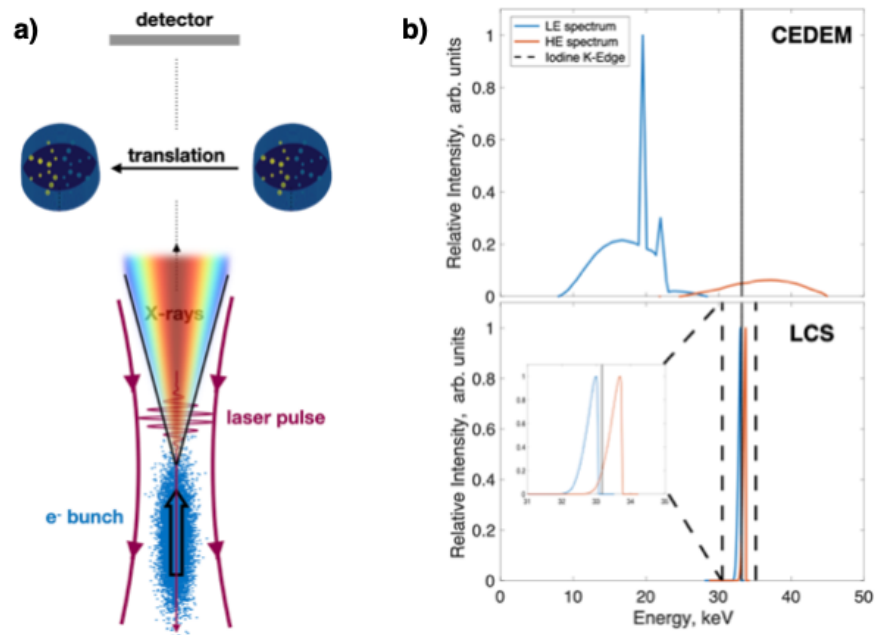


Figure 3. a) Depiction of scanning K-edge subtraction setup using a LCS source. The object will be scanned through the beam thereby exposing it to energies that are both above and below the K-edge. b) Comparison of LCS spectrum to a clinically available CEDEM source. LCS has much more narrow bandwidths that are much more suited for K-edge subtraction imaging.

2. METHODS

In order to accurately simulate a LCS source, a multistep simulation pathway was developed starting from the electron beam to sampling of the scattered x-ray spectrum.

2.1 Simulation of the electron beam

The electron beam was simulated using General Particle Tracer (GPT) code. This beam was simulated to mimic the expected output of an 11.424 GHz X-band linear accelerator (LINAC) that is currently under construction at Luminon Technologies, Inc. [10]. This electron beam consists of a micro-bunch charge of 25 pC, mean electron energy between 25 MeV and 100 MeV, electron energy spread of 0.03%, beam emittance of 0.2 mm mrad, electron bunch length of 2 ps and a root-mean-square (RMS) spot size of 5 microns. The phase space of this electron beam was then gathered to be used in the calculation of the LCS interaction.

2.2 Calculation of the laser-Compton scattering x-ray spectrum

The LCS interaction between the laser pulse and electron bunch was computed using a Mathematica notebook. The laser pulse was approximated by using a plane wave that is gaussian in time with a Rayleigh range sufficient to interact with

the 2 ps electron bunch duration. The wavelength of the laser was set to 354 nm. The electron beam phase space was used as input to the notebook and the following spectrum that is double differential in energy and angle was computed [6,11].

$$\frac{dN}{d\omega d\Omega} = \int \frac{d\sigma}{d\Omega} \delta(\omega - \omega_l) (1 + \beta_0) n_l(x_\mu) n_e(x_\mu) dx_\mu \quad (2)$$

Here, $\frac{d\sigma}{d\Omega}$ is the Klien-Nishina differential cross section, ω and ω_l are respectively the frequencies of the scattered X-ray and the laser, n_l and n_e are the laser and electron shape functions that are functions of the electron 4-position x_μ . The notebook outputs a 4-dimensional array with values for the scattered x-ray angle in x, angle in y, energy and intensity. This calculation was performed for 3 different energy tunings of the electron beam and used as input into *Compton FastFit* [12] to quickly scan over electron energy during optimization.

2.3 X-ray propagation and Bayesian optimization routine

X-ray propagation through a computational phantom was computed using a Beer-Lambert method described previously [10]. This method is fast decreasing computation time and is accurate to established Monte Carlo code within 0.15% accuracy in signal and 1% in noise. The propagation routine takes a LCS spectral input generated from *FastFit* and generates an image of the phantom. From here, the image is analyzed by taking the contrast-to-noise ratio (CNR) of the respective inserts. These values are fed to a Bayesian optimization routine that evaluates the following objective function modified from what was previously used for this specific problem [10].

$$Obj = \arg \max_{\gamma, \mathbf{r}} \left[\left(\min_i CNR_i(\gamma) \right) \sum_i \frac{CNR_i(\gamma)}{CNR_i(\gamma_{max})} \left| \int f(E; \gamma, \mathbf{r}) dE \right| \right] \quad (3)$$

This Bayesian routine then returns an estimate of the electron beam Lorentz factor, γ , and other optimizable parameters to generate a new spectrum for x-ray propagation. The cycle of *FastFit* – x-ray propagation – Bayesian algorithm was performed using Matlab and continued for a maximum of 325 steps or until the objective function was sufficiently maximized. Figure 4 shows an example visualization of the Bayesian optimization in two of the optimizable dimensions. The other optimizable parameters used were the inner and outer radii of the annular exclusion zone.

2.4 Computational phantom

The computational phantom was a 4.2 cm thick mammography phantom that has been used in a previous gadolinium study [10]. The phantom was designed to accurately simulate K-edge subtraction mammography. It contains inserts that represent tumors suspended in a fibroglandular and adipose tissue medium with varying ratios between the two tissue types. Iodine replaced the gadolinium inserts in concentrations of 0.2 and 0.1 mass percent.

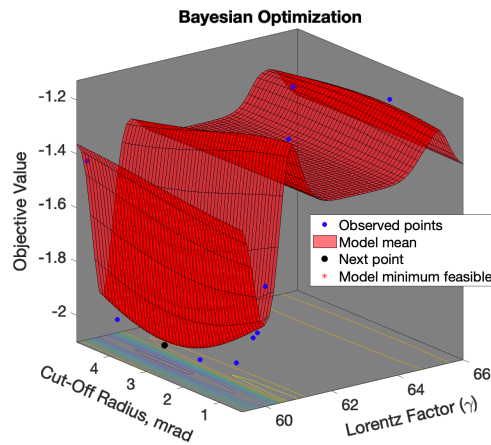


Figure 4. Sample visualization of the first 10 steps in a Bayesian optimization routine used in this paper. The optimized parameters shown here are the Lorentz factor and the radius of exclusion. This implementation minimizes the negative of the objective function.

3. RESULTS AND DISCUSSION

Since it is known that there is some small energy bandwidth at every location in space, there may exist a zone that should be excluded to obtain isolated energy spectra that are above and below the K-edge. Additionally, since the mean energies are circular in space (see Figure 1b), circular regions were used for above/below spectra Bayesian optimization of the LCS source. More specifically, a circular annulus was denoted as an exclusion zone to optimize. The parameters to be optimized were the mean Lorentz factor of the electron beam (converted the Compton edge energy of the scattered radiation in the following figures) and the inner/outer radii of the circular annulus exclusion zone.

Figure 5 shows the iterative result of the Bayesian optimization up to 325 steps. After only 10 iterations, a reasonably optimized solution was found. While in less than 50 iterations, a fully optimized solution was obtained. The simulation was allowed to continue beyond that to allow it to sample more of the parameter space. X-ray propagation is the most time-consuming step of the algorithm, which takes approximately 12 minutes per step at the resolution of the phantom and computational resources used in this study. This means that a reasonable solution can be obtained in just two hours which is substantially faster than a full parameter space scan which scales as n^m where m is the number of parameters and n is the number of samples per parameter. For example, if this problem were split into a *coarse* 20 steps each, that would be $20^3 = 8,000$ steps and take 67 days to complete. Adding just one or two more parameters would quickly reach computational intractability, marking the usefulness of a Bayesian optimization routine. An added advantage of the Bayesian algorithm is that if let run for more iterations, like done here, it will begin to sample more of the parameter space thereby enabling some confidence if the optimum is truly global as opposed to a local one.

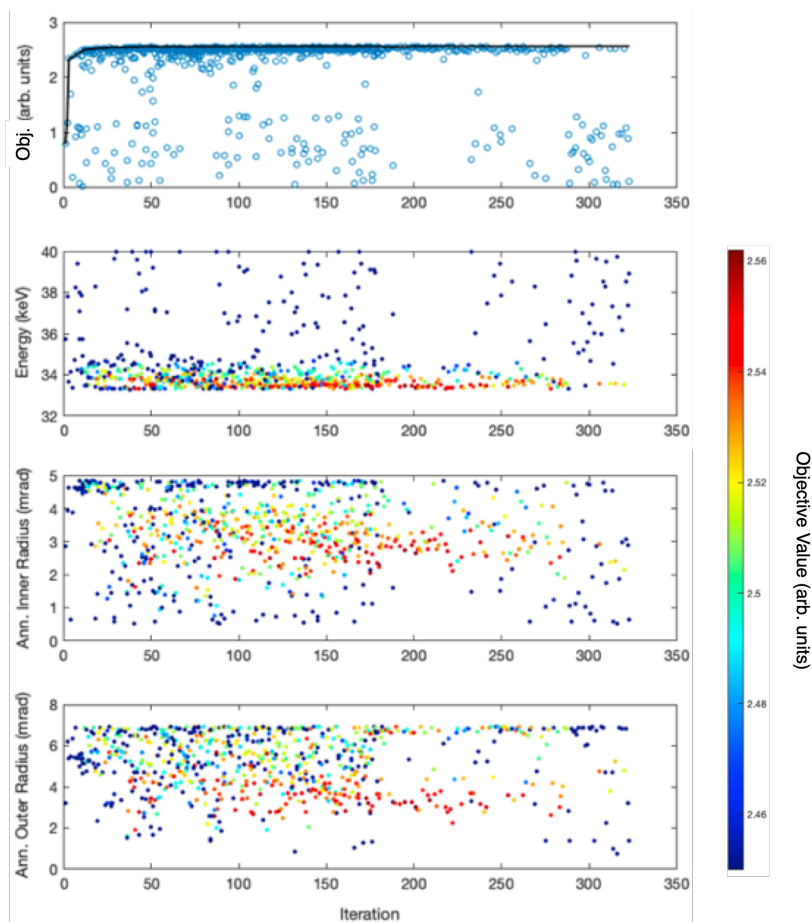


Figure 5. Results from Bayesian optimization during a 325-iteration run for SKES using a LCS x-ray source. The most optimal parameters were found to be a Compton edge energy of approximately 34 keV, inner annulus radius of 2.8 mrad and outer annulus radius of 3.5 mrad.

Figure 6 shows the results on how the Bayesian optimized parameters compare to other methods. The left column in the figure shows the spatial spectrum, integrated energy spectrum, and phantom image we would get resulting from a SKES simulation from drawing a circle that contains energies that are only above the K-edge of iodine, while everything outside of the circle is taken to be a below spectrum. This is compared to the second column that uses the Bayesian optimized parameters that increases the annular exclusion zone from zero to a finite size. The Bayesian optimized simulation resulted in a much better signal at the locations of the iodine within the phantom.

The authors were also interested in how the Bayesian optimized SKES imaging technique compares to a dual-energy tuning method described previously [10]. The third column of Figure 6 shows the images generated with the mammographic phantom. The mean CNR of the large inserts on the top half of the phantom were used to compare the image quality between the two. The CNR of the dual-energy tuning method was 2.65 and the CNR for the scanning method was very similar at 2.67, showing the non-inferior image quality between the two methods. This shows support that this scanning method, which is uniquely enabled by the angular correlation of a LCS source, can be used for KES imaging.

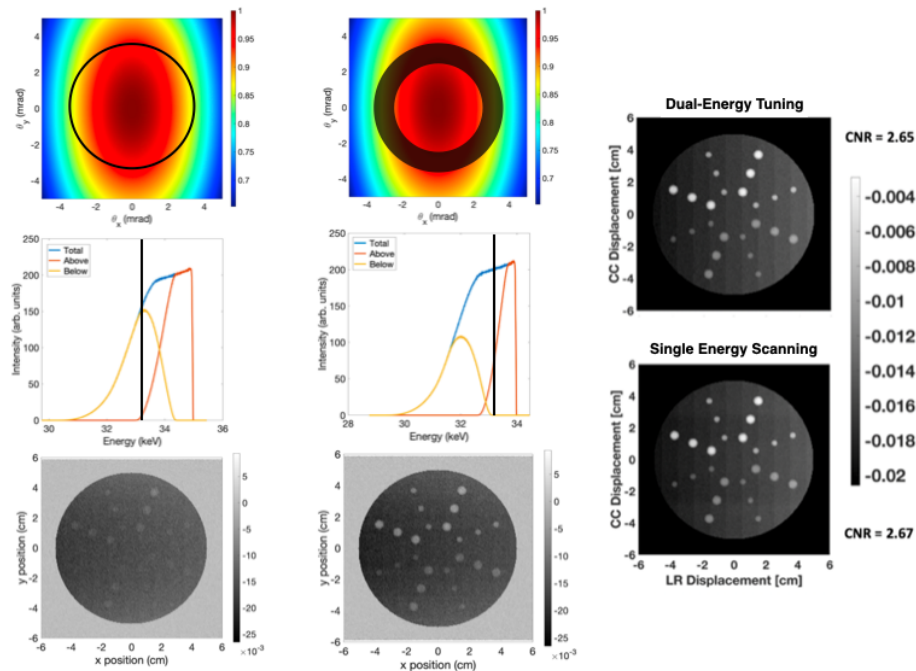


Figure 6. Left Column) X-ray spatial intensity profile, total integrated x-ray spectrum, and phantom SKES image using heuristically drawn circle with all photons in the center region are above the K-edge energy of iodine. Center Column) X-ray spatial intensity profile, total integrated x-ray spectrum, and phantom SKES image using Bayesian optimized parameters for the Lorentz factor and exclusion zone radii. Right Column) Comparison of SKES to a prior dual-energy tuning LCS method described previously; area outside of the phantom was set to black in this case for clarity at the phantom. Colorbars for the images of the phantoms are signal with arbitrary units. Colorbars for the spatial intensity profiles are relative intensity with arbitrary units.

4. CONCLUSION

A Bayesian optimization routine was used to quickly and accurately determine the optimal laser-Compton scattering source parameters for an application of scanning K-edge subtraction imaging. The routine was able to find an optimized set of parameters in only a fraction of the time it would take to scan the entire n^m parameter space. The optimized spectrum generated an image that had better quality for tumor detection in a mammographic phantom compared to an idealized use case. Moreover, the Bayesian algorithm aided in the demonstration that scanning LCS-KES can generate the same image quality compared to its dual-energy tuning counterpart.

REFERENCES

- [1] Paternò, G., Cardarelli, P., Gambaccini, M., Serafini, L., Petrillo, V., Drebot, I., & Taibi, A. (2019). Inverse Compton radiation: a novel x-ray source for K-edge subtraction angiography?. *Physics in Medicine & Biology*, 64(18), 185002.
- [2] Kulpe, S., Dierolf, M., Günther, B., Busse, M., Achterhold, K., Gleich, B., ... & Pfeiffer, D. (2019). K-edge subtraction computed tomography with a compact synchrotron X-ray source. *Scientific reports*, 9(1), 13332.
- [3] Yamada, K., Kuroda, R., Toyakawa, H., Ikeura-Sekiguchi, H., Yasumoto, M., Koike, M., Sakai, F., Mori, K., Mori, H., Fukuyama, N. and Sato, E. (2009). A trial for fine and low-dose imaging of biological specimens using quasi-monochromatic laser-Compton X-rays. *Nuclear Instruments and Methods in Physics Research Section A: Accelerators, Spectrometers, Detectors and Associated Equipment*, 608(1), pp.S7-S10.
- [4] Gibson, D.J., Albert, F., Anderson, S.G., Betts, S.M., Messerly, M.J., Phan, H.H., Semenov, V.A., Shverdin, M.Y., Tremaine, A.M., Hartemann, F.V. and Siders, C.W. (2010). Design and operation of a tunable MeV-level Compton-scattering-based γ -ray source. *Physical Review Special Topics-Accelerators and Beams*, 13(7), p.070703.
- [5] Albert, F., Anderson, S.G., Gibson, D.J., Marsh, R.A., Wu, S.S., Siders, C.W., Barty, C.P.J. and Hartemann, F.V. (2011). Design of narrow-band Compton scattering sources for nuclear resonance fluorescence. *Physical Review Special Topics-Accelerators and Beams*, 14(5), p.050703.
- [6] Albert, F., Anderson, S.G., Gibson, D.J., Haggmann, C.A., Johnson, M.S., Messerly, M., Semenov, V., Shverdin, M.Y., Rusnak, B., Tremaine, A.M. and Hartemann, F.V. (2010). Characterization and applications of a tunable, laser-based, MeV-class Compton-scattering γ -ray source. *Physical Review Special Topics-Accelerators and Beams*, 13(7), p.070704.
- [7] Jochelson, M.S., Dershaw, D.D., Sung, J.S., Heerdt, A.S., Thornton, C., Moskowitz, C.S., Ferrara, J. and Morris, E.A. (2013). Bilateral contrast-enhanced dual-energy digital mammography: feasibility and comparison with conventional digital mammography and MR imaging in women with known breast carcinoma. *Radiology*, 266(3), pp.743-751.
- [8] Barty, C.P.J. (2015). Methods for 2-color radiography with laser-Compton x-ray sources. US Patent #US10508998B2.
- [9] Effarah, H.H., Reutershan, T. and Barty, C.P.J. (2022, March). Scanning K-edge Subtraction Imaging is Enabled by the Angle-correlated Spectra of Laser Compton X-ray Sources. In *Compact EUV & X-ray Light Sources* (pp. EW4A-4). Optica Publishing Group.
- [10] Reutershan, T., Effarah, H.H., Lagzda, A. and Barty, C.P.J., 2022. Numerical evaluation of high-energy, laser-Compton x-ray sources for contrast enhancement and dose reduction in clinical imaging via gadolinium-based K-edge subtraction. *Applied Optics*, 61(6), pp.C162-C178.
- [11] Hartemann, F.V., Brown, W.J., Gibson, D.J., Anderson, S.G., Tremaine, A.M., Springer, P.T., Wootton, A.J., Hartouni, E.P. and Barty, C.P.J., 2005. High-energy scaling of Compton scattering light sources. *Physical Review Special Topics-Accelerators and Beams*, 8(10), p.100702.
- [12] Effarah, H.H., Reutershan, T., Lagzda, A., Hwang, Y., Hartemann, F.V. and Barty, C.P.J., 2022. Computational method for the optimization of quasimonoenergetic laser Compton x-ray sources for imaging applications. *Applied Optics*, 61(6), pp.C143-C153.